*EVS26*
*Los Angeles, California, May 6 - 9, 2012*

# Effect of Gear Shift and Engine Start Losses on Control Strategies for Hybrid Electric Vehicles

V. Ngo[1*], T. Hofman[1], M. Steinbuch[1], A. Serrarens[2]
[1](*corresponding author) Eindhoven University of Technology,
PO Box 513, 5600 MB Eindhoven, The Netherlands;
email: {d.v.ngo, t.hofman, m.steinbuch}@tue.nl
[2]Drivetrain Innovations B.V., Croy 46, 5653 LD Eindhoven, The Netherlands;
email: serrarens@dtinnovations.nl

**Abstract**

In this paper, energetic loss models in the events of shifting gear and starting engine in a parallel Hybrid Electric Vehicle equipped with an Automated Manual Transmission (AMT) will be introduced. The optimal control algorithm for the start-stop, power split and gear shift problem based on Dynamic Programming-Pontryagin's Minimum Principle control approach is used to evaluate the effect of gear shift and engine start losses on the optimal solution. Furthermore, with preview route information available, a model predictive control algorithm is utilized to investigate the achievable fuel savings with respect to the prediction horizon. Under influence of the gear shift loss, simulation results of the prototype hybrid passenger car disclose a superior fuel efficiency property of the powershift AMT over its normal AMT counterpart. Sensitivity analysis of the traction force interruption time in a gear shift process can give a new perception on fuel economy benefit of powershift transmissions (e.g. automatic, dual clutch, powershift AMT, etc.) over a normal AMT. The study also reveals a minimum prediction length of 4s required for the design of such a realtime implementable controller to get the possible maximum fuel economy level under the impact of the engine start loss.

*Keywords: gear shift loss, engine start loss, hybrid electric vehicle, dynamic programming-Pontryagin's minimum principle, model predictive control.*

## 1 Introduction

Design of the Energy Management Strategies (EMSs) for Hybrid Electric Vehicles (HEVs) in general aims at optimally choosing the power split between the internal combustion engine and the electric machine to improve fuel economy, [1–15]. For full HEVs equipped with discrete ratio transmissions, e.g. Automated Manual Transmission (AMT), the operating points of the hybrid powertrain are not only defined by the power split but also by the start-stop state and the gear position. Hence, by further optimizing the start-stop and gear shift strategies, fuel economy of the vehicle is improved substantially compared to the EMSs optimizing only the power split. Consequently, the controller allows: i) the transmission to shift earlier and at higher frequency; ii) the engine to stop and restart more frequently, for fuel economy benefits, see in [1,2,6–14]. For each event of gear shift or engine start, there is an amount of energy loss. So, it is worth to concern these losses when the number of shifts and starts is at considerable amount for a certain drive cycle. However, none of the mentioned published papers has been addressing the relevant gear shift and engine start losses, and thus analyzing their effects on the control strategies of the vehicles. Therefore, this study will focus on these issues.

Regarding to the gear shift, a shift decision will encounter a change of the engine rotating dynamics, a possible clutch operation loss and a con-

sequent vehicle velocity loss due to interrupted traction torque. Hence, any later compensation for the earlier gear shift loss might cost additional fuel. For a decision of restarting the engine, apart from the traction torque required at the wheels, an extra torque from the electric machine is needed for cranking up the engine from stand still and compensating the friction loss in clutch. This would consume an amount of electric energy which sometime later can cost the fuel for recharging. Engine combustion takeover after the cranking phase for each engine start process should also be considered. In summary, on highly dynamic drive cycles with high frequent stop-go patterns, the number of gear shifts and engine starts will increase and thus the fuel consumption might increase.

Therefore, this study will bring the aforementioned aspects, regarding the losses of shifting the gear and starting the engine, into the EMS [1] to analyze their influences on fuel economy. It's worth to mention that the proposed EMS for a parallel HEV equipped with an AMT, optimally control not only the power split but also the engine start-stop and gear shift. The control method based on a combination of Dynamic Programming (DP) and Pontryagin's Minimum Principle (PMP), so-called DP-PMP, improves the fuel economy significantly and possesses a fast computation maner, and thus suitable for the purpose of this study. First of all, a sensitivity study of fuel economy with respect to the gear shift command is conducted towards a gear shift hysteresis strategy implementation to get rid of the shift busyness and haunt. A gear shift loss model capturing the main shifting characteristics is introduced and incorporated in the EMS for fuel economy evaluation. Then, a sensitivity study of the traction torque interruption time during a gear shift process can reveal a new perception of fuel efficiency advantage of powershift transmissions compared to non-powershift counterparts as applied in commercial vehicles. In addition, an engine start loss model corresponding to the prototype HEV is built and considered in the EMS design to reflect its effect on fuel consumption. Model Predictive Control (MPC) for the HEV, [2], appears to be a possible candidate for realtime implementation when using preview route information. Therefore, the impact of prediction horizon length on the achievable fuel savings of the HEV under the engine start loss is necessary to be investigated for such a realtime implementable control algorithm.

The content of this paper is organized as follows. The hybrid powertrain model is given in Section 2. The optimal control problem for the engine start-stop decision, the power split and the gear shift is introduced in Section 3. Gear shift loss model and its influence on the fuel economy will be discussed in Section 4. Engine start loss model and the related control problem are addressed in Section 5. Prediction horizon length sensitivity study on fuel economy resulted from the corresponding predictive control algorithm under the impact of engine start loss is given in Section 6. Finally, the conclusions are given in Section 7.

## 2 Hybrid Powertrain Model

Aiming at deriving an EMS, the quasi-static models of the powertrain components are used and simulated with a time step of one second. The system dynamics faster than $1Hz$ are ignored [23]. The clutch system is considered as a discrete switch to connect and to disconnect the engine immediately to and from the driveline. The energy losses during the clutching process of gear shift and engine start are addressing explicitly in the section 4 and 5 respectively.

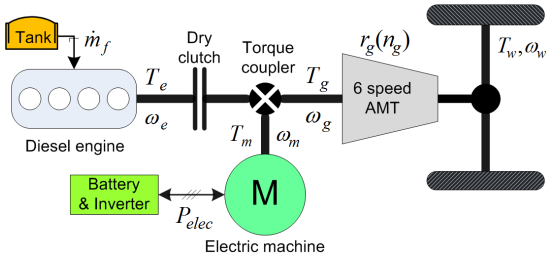


Figure 1: A parallel hybrid electric vehicle topology.

The start-stop system can be modeled by using a discrete state variable $s_e(k)$ to represent the engine on-off state.

$$s_e(k) = \begin{cases} 1 & \text{if engine on,} \\ 0 & \text{if engine off.} \end{cases} \tag{1}$$

We ignore the engine drag torque during deceleration phase due to the disconnection of engine from the driveline and engine shut down. For a certain engine speed $\omega_e(k)$, the fuel consumption model is approximated as an affine piecewise second order function of the engine power $P_e(k)$. The fit coefficients $a_0, a_1, a_2$ are dependent on engine speed.

$$\dot{m}_f\big(P_e(k), k\big) \approx \big(a_0 P_e^2(k) + a_1 P_e(k) + a_2\big) s_e(k). \tag{2}$$

The electric machine efficiency $\eta_m$ is assumed to be constant. Therefore the power $P_m(k)$ flowing in and out of the electric machine in motoring mode and generating mode is expressed as follows.

$$\begin{aligned} P_m(k) &= \eta_m P_{elec}(k) \quad \text{(if motoring);} \\ P_m(k) &= \frac{1}{\eta_m} P_{elec}(k) \quad \text{(generating).} \end{aligned} \tag{3}$$

We assume the battery state of energy $e_s(k)$ to be in a nominal range $[E_{s,min}, \quad E_{s,max}]$ such that its effect to the efficiency model can be ignored. Hence, the electrical power $P_{elec}(k)$ can be approximated as a quadratic function of the chemical power $P_s(k)$ as

$$P_{elec}(k) \approx b_0 P_s^2(k) + b_1 P_s(k) + b_2. \tag{4}$$

The gearbox efficiency model is assumed to be constant $\eta_g$ for all gears. The torque and speed relations in the driveline of hybrid electric vehicle are given by

$$T_w(k) = T_g(k) r_g\big(n_g(k)\big)\eta_g, \tag{5}$$

$$\omega_w(k) = \frac{\omega_m(k)}{r_g\big(n_g(k)\big)}, \quad \omega_m(k) = \omega_g(k). \tag{6}$$

where $T_w(k)$ is the transferred torque at the wheels (assumed equal to output torque of the transmission); $T_g(k)$ is the input torque of the transmission; $r_g\big(n_g(k)\big)$ denotes the discrete gear ratio depending on the gear position $n_g(k)$; $\omega_w(k)$ is the wheel speed; $\omega_m(k)$ is the electric machine speed and $\omega_g(k)$ is the transmission input speed.
At any time step $k$, the power flow equilibrium in the parallel hybrid powertrain topology is expressed as

$$P_e(k) = P_g(k) + P_m(k). \tag{7}$$

with $P_g(k)$ is the power flow at the transmission input.

# 3 Hybrid Powertrain Control Algorithm

## 3.1 Optimal Control Problem Formulation

Given a drive cycle $v(k)$ with time length of $N$, find an optimal control law $u^*(k) = \big[u^*_{se}(k),\ P^*_e(k),\ u^*_g(k)\big]$, which are the optimal control variables for battery state of energy, start-stop system and gear shifting respectively, that minimize the fuel cost functional $J$ described by

$$J = \sum_{k=0}^{N-1} \dot{m}_f\big(P_e(k), \omega_e(k), k\big)\Delta t, \tag{8}$$

subject to:

*1.* the hybrid powertrain dynamics,

$$s_e(k+1) = s_e(k) + u_{se}(k), \tag{9}$$

$$e_s(k+1) = e_s(k) + P_s(k)\Delta t, \tag{10}$$

$$n_g(k+1) = n_g(k) + u_g(k). \tag{11}$$

*2.* the constraints on the speeds of the drivetrain components,

$$\omega_{e,min} \ \leq \ \omega_e(k) \ \leq \ \omega_{e,max}, \tag{12a}$$

$$0 \ \leq \ \omega_m(k) \ \leq \ \omega_{m,max}, \tag{12b}$$

*3.* the constraints on the engine power $P_e(k)$, the electric machine power $P_m(k)$ and the battery power $P_s(k)$ are,

$$0 \ \leq \ P_e(k) \ \leq \ P_{e,max}\big(\omega_e(k)\big), \tag{13a}$$

$$P_{m,min}\big(\omega_m(k)\big) \leq P_m(k) \leq P_{m,max}\big(\omega_m(k)\big), \tag{13b}$$

$$P_{s,min} \ \leq \ P_s(k) \ \leq \ P_{s,max}, \tag{13c}$$

*4.* the constraints on the system states, which are start-stop state and gear position,

$$0 \ \leq \ s_e(k) \ \leq \ 1, \tag{14}$$

$$1 \ \leq \ n_g(k) \ \leq \ 6, \tag{15}$$

with notice that the constraints on the engine on-off state are described by (1),
*5.* the designed constraints at the end of the drive cycle,

$$e_s(N) = e_s(0) + \sum_{k=0}^{N-1} P_s(k)\cdot\Delta t = e_s(0), \tag{16}$$

*6.* the constraints on the control variables,

$$u_{se}(k) = \begin{cases} [0,\ 1] & \text{if} \quad s_e(k) = 0, \\ [-1,\ 0] & \text{if} \quad s_e(k) = 1. \end{cases} \tag{17}$$

$$u_g(k) \in \big\{u_{g,min}, \cdots, -1, 0, 1, \cdots, u_{g,max}\big\}, \tag{18}$$

wherein: $\Delta t$ is the time step of the discrete system; $u_{g,min}$ and $u_{g,max}$ are the lower and upper bounds for the gear shift command $u_g(k)$.
In this study, the upper and lower bounds of the state variable $e_s(k)$ are ignored by assumption that the battery capacity is chosen properly such that it never exceeds its bounds for increasing lifetime and reliable operation. Battery operating temperature is assumed to be under tight control.

## 3.2 Dynamic Programming-Pontryagin's Minimum Principle Control Approach

DP-PMP control approach appears to be a good candidate to solve the formulated optimal control problem. For further details of this approach, interested readers are referred to [1]. In summary, DP is used in the outer loop to define the optimal gear position and engine on-off state for the whole drive cycle. PMP is used in the inner loop to define the instantaneous optimal solution of engine power at every time step with a certain gear position and engine state.

### 3.3 Gear Shift Command Sensitivity

From (11), the bounds of the gear shift command $u_g(k)$ determine the dynamic behavior of the next gear position $n_g(k+1)$, which eventually affects to the fuel economy of the vehicle. From (18), $u_{g,min}$ and $u_{g,max}$ are varied to investigate the sensitivity of the optimal solution with respect to gear shifting dynamics. With a 6-speed transmission, the upper bound and the lower bound on $u_g(k)$ are 5 and -5 respectively which leads to five main cases of consideration as in (19).

$$\begin{bmatrix} u_{g,min} \\ u_{g,max} \end{bmatrix} \in \left\{ \begin{bmatrix} -1 \\ 1 \end{bmatrix}, \begin{bmatrix} -2 \\ 2 \end{bmatrix}, \begin{bmatrix} -3 \\ 3 \end{bmatrix}, \begin{bmatrix} -4 \\ 4 \end{bmatrix}, \begin{bmatrix} -5 \\ 5 \end{bmatrix} \right\} \tag{19}$$

The drive cycles chosen for testing the control algorithm are NEDC, FTP75, LA92 and CADC to represent real driving scenarios. Simulation results of fuel consumption for the case $[u_{g,min};\ u_{g,max}] = [-1;\ 1]$ are shown in Table 1. Compared to this case, the relative fuel economy of the other cases mentioned in (19) is very small ($\approx 0\%$). This means that increasing the bounds on the gear shift command does not affect fuel economy of the vehicle under control. Or, in other words, choosing $u_g(k) \in \{-1, 0, 1\}$ is the optimum gear shift command in terms of the fuel economy and the engine speed variation reduction during shifting.
Depicted in Fig. 2 are the graphical results for NEDC, the gear shifting pattern, engine on-off state and battery state of energy are almost the same for five cases in (19) which further demonstrates robustness of the controlled powertrain system under uncertainty of the gear shift command bounds.

Table 1: Fuel consumption with gear shift command bounds: $[u_{g,min};\ u_{g,max}] = [-1;\ 1]$.

| Cycle | NEDC | FTP75 | LA92 | CADC |
|---|---|---|---|---|
| Fuel [g] | 300.5 | 480.3 | 530.8 | 1873.9 |

### 3.4 Gear Shift Hysteresis

The proposed control strategy allows the transmission to shift as much as possible with maximum shift frequency (equal to the frequency of the discrete powertrain system) for fuel savings. Actually, vehicles equipped with an AMT can only shift the transmission under the respect of so-called shift hysteresis to prevent the shift haunting, i.e. shifting two times at two consecutive time steps and shifting back and forth, and avoid losing the driveability. This practical issue

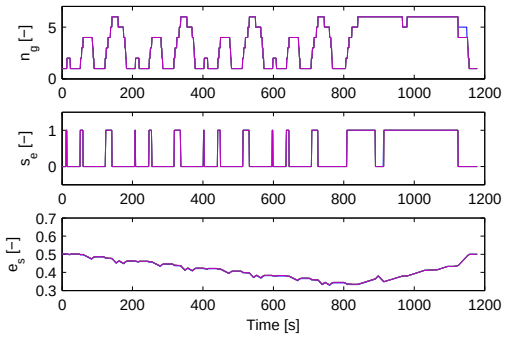


Figure 2: Sensitivity study on the bound gear shift command $u_g$.

can be implemented into the EMS by imposing a constraint of not changing gear within $n_{hys}$ time steps after each previous shifting, described by a general shift condition,

*general shift condition*

$u_{hys} = u_g(k - n_{hys}) + \cdots + u_g(k-1)$;
if $u_{hys} == 0$
$u_g(k) \in \{-1, 0, 1\}$,
else
$u_g(k) = 0$,
end

This means that a gear shift decision can only make when a hysteresis time $n_{hys}$ is respected. The powertrain dynamic system for control will increase in dimension by an order of $n_{hys} - 1$. Therefore, $n_{hys} > 1$ will make the control system more complicated and affect to the computation load of the control algorithm. Hence, in this study $n_{hys} = 1$ is adopted for a reasonable compromise, which leads a simplified shift hysteresis condition as in (20),

$$u_g(k-1)u_g(k) = 0. \tag{20}$$

Table 2: Gear shift hysteresis study.

| Cycle | Baseline | | Shift Hysteresis | |
|---|---|---|---|---|
| | Fuel [g] | No. shift | Fuel [g] | No. shift |
| NEDC | 300.5 | 73 | 301.8 (0.4%) | 71 (-2.7%) |
| FTP75 | 480.3 | 423 | 481.5 (0.3%) | 197 (-53.4%) |
| LA92 | 530.8 | 358 | 531.8 (0.2%) | 179 (-50%) |
| CADC | 1873.9 | 651 | 1876.2 (0.1%) | 244 (-62.5%) |

Simulation results are shown in Table 2. The relative fuel differences between the shift hysteresis case and the baseline are indicated in the parenthesis. It depicts that the gear shift hysteresis strategy reduces the number of shift significantly, meanwhile the fuel economy impact is small. The obtained results reveal the essential role of shift hysteresis in removing the unnecessary shifts which do not affect the fuel economy considerably.

# 4 Gear Shift Loss Model and Control Problem

The gear shift process of an AMT-based vehicle includes three chronological phases: 1) disengaging the clutch; 2) shifting the transmission to the expected gear; 3) and engaging the clutch. The speed and torque profiles of both clutch and engine during the shifting process are assumed to be properly controlled in every phase to ensure quick shifting, more comfort and and less friction losses, etc., [18, 25]. The energetic loss model involved with a gear shifting process is described in the next section.

## 4.1 Gear Shift Loss Model

A decision of shifting the gear is meaningful when the vehicle is in acceleration or cruising modes wherein the engine is used as a primary mover to meet the required positive driving torque at the wheels. Transmission can be shifted up to accommodate the engine speed to the vehicle speed changed for fuel economy, or even shifted down, called kick-downshift, if higher acceleration required or driving uphill.
During electrically driving mode (the electric machine is used to solely propel the vehicle) or deceleration mode (electric machine operates as a generator to recuperate the kinetic energy), hybrid powertrain with the available start-stop functionality can turn the engine off and disconnect it from the driveline. Apparently, there is no slippage phenomena in clutch which leads to no energy loss involved. Gear shifting during these driving modes can be assumed to occur immediately.
In summary, only upshift and kick-downshift events are under concern with the corresponding gear shift loss models as follows.

### 4.1.1 Upshift loss

Fig. 3 demonstrates the simplified uniform profiles of speed and torque of engine and clutch in an upshift process. Three phases of the shifting process are indicated. The whole shifting period, on average, can be assumed to be equivalent to the time step of the EMS, $\Delta t_{shift} = \Delta t$, see [18–20, 25].
In phase 1 (disengagement) & 3 (engagement), engine torque and clutch transferred torque are controlled to have a declined and inclined patterns to allow comfort disengagement and engagement respectively. Hence, there exists slip phenomena at the clutch to transfer traction force to the wheels during these phases. The speed difference between both sides of the clutch are not large such that an equality of engine and clutch speeds can be assumed as a simplification. In phase 2, the clutch is fully disengaged for shifting the gear and there is a traction force interruption which finally results in a velocity loss for an interval $\Delta t_{int}$. Due to the engine drag torque, engine speed is assumed to reduce to a synchronization point corresponding to the clutch speed at the next higher gear.

- phase 1 & 3, the engine torque can be averagely approximated as

$$T_{e,slip} = \frac{T_e}{2} \tag{21}$$

- in phase 2, the engine torque

$$T_{e,int} = 0 \tag{22}$$

- average traction power incurred during a upshifting process due to clutch slipping

$$P_{e,slip} = T_{e,slip}\omega_e \frac{\Delta t_{shift} - \Delta t_{int}}{\Delta t_{shift}} \tag{23}$$

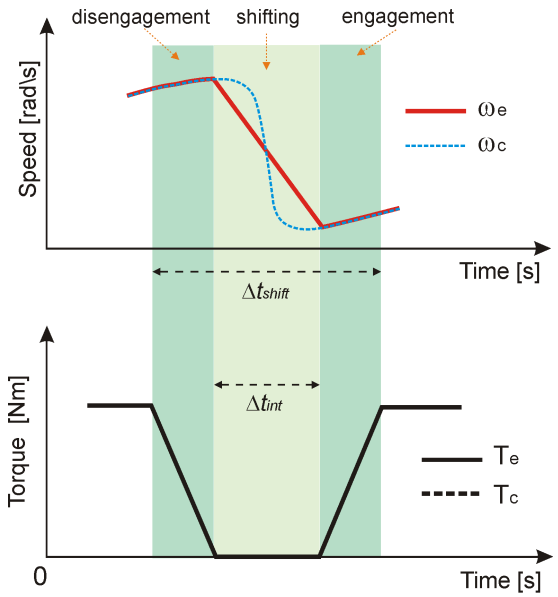


Figure 3: Simplified engine and clutch profiles for a gear upshift.

### 4.1.2 Kick-downshift loss

Fig. 4 shows the typical profiles of engine and clutch torque for a kick-downshift process, see [18–20, 25]. It also consists of three

phases. The clutch torque is zeros for the shifting phase. Meanwhile the engine torque is maintained above zero to increase the engine speed up to the synchronization point corresponding to the clutch speed at the next lower gear. Hence the engine torque model can be described as

- in phase 1 & 3, the engine torque,

$$T_{e,slip} = \frac{T_e + T_{e,int}}{2}. \tag{24}$$

- in phase 2, the engine torque

$$T_{e,int} = J_e \frac{\omega_c - \omega_e}{\Delta t_{int}}, \tag{25}$$

  where $J_e$ is the equivalent inertia on the engine side (seen from clutch); $\omega_e$ is the engine speed before shifting; $\omega_c$ is the clutch speed after shifting.

- average traction power incurred during a kick-downshift process due to clutch slipping

$$P_{e,slip} = T_{e,slip}\omega_e \frac{\Delta t_{shift} - \Delta t_{int}}{\Delta t_{shift}} \tag{26}$$

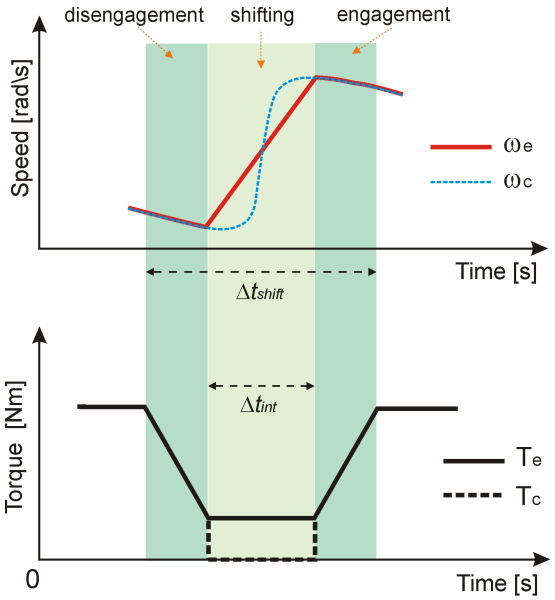


Figure 4: Simplified engine and clutch profiles during a gear kick-downshift.

### 4.1.3 Velocity tracking loss

as similar to the analysis above, the vehicle traction force is totally lost during the phase 2 of a gear shift process. During the phases 1 & 3, traction force is partially lost due to clutch slipping requirement for gear change. Taking all these traction force characteristics into account will results in an velocity loss for each gear upshift or kick-downshift. Therefore, the vehicle needs to accelerate more, later in the driving mission, in order to compensate for the loss in each gear shift. This will influence to the fuel economy evaluation of the vehicle.
Apparently, the length of the power interruption in phase 2, denoted by $\Delta t_{int}$, mainly decide the effect level of gear shift loss on the vehicle performance. In reality, the interruption time $\Delta t_{int}$ is varied according to the types of vehicles and the clutch operation conditions [18, 25]. Therefore, sensitivity study with respect to $\Delta t_{int}$ should be done for thorough analysis of gear shift loss effect.

## 4.2 Optimal Control Problem with Gear Shift Loss

Design of the EMS for AMT-based HEVs always assumes the gear shift can occurs immediately, which means that there is no torque interruption at the wheels when shifting and the vehicle keeps tracking the driving profile. This is only true when the transmission possesses the power-shift technology, see [25] for example, to enable the traction force to be transferred to the wheel during shifting. In reality, the consequence of a gear shift activity is a loss of vehicle speed tracking. To fulfill the required traveled distance at the final destination, the vehicle must accelerate more after each gear shift to compensate for the velocity loss during shifting.
As shown in section 3.4, the optimal control strategy for HEV yields many shifts for fuel economy improvement. Therefore, it's a fair evaluation of the gear shift contribution to fuel benefit when having the gear shift loss model incorporated in the EMS. As a consequence of velocity tracking loss, the vehicle could not follow a prior drive cycle, and thus the next vehicle speed is gear position dependent. An EMS optimizing further the driving profile (velocity, traveled time) [21, 22] is an appropriate solution for the control problem with the gear shift loss model involved. Such a control algorithm is complicated and out of scope of this study. In order to cope with velocity tracking loss, an appropriate approach to fairly investigate the effect of gear shift loss model on the fuel economy and evaluate the trait of powershift property is introduced as follows.
*Powershift AMT*: the EMS is designed with no gear shift loss model taken into account. This means the AMT has the powershift technology to ensure the velocity tracking. Gear shift can be performed instantly. The designed EMS optimizes the engine on-off state, power split and gear shift.
*Normal AMT*: the hybrid powertrain is equipped with an normal AMT. The gear shift loss model is respect during the design process of the EMS. The optimal gear shift strategy obtained from the powershift AMT is now used as an prescribed one for the normal AMT. To ensure the same average speed with the powershift AMT for a fair

comparison on fuel economy, the next vehicle speed is controlled by an integral regulator. The powertrain is simulated in forward-facing manner and the EMS optimizes the engine on-off state and power split.

### 4.3 Simulation results

The gear shift hysteresis strategy is taken into account in the case of the powershift AMT to avoid any gear shifting haunting pattern. Fig. 5 depicts the zoom-in of one part of simulation results on NEDC. It can be seen that when an upshift occurs, acceleration is lost during the gear shift process for the case of the normal AMT, see the red dotted line. Right after each gear shift, a higher acceleration compared with the powershift AMT is required to compensate for the loss during the gear shift before.

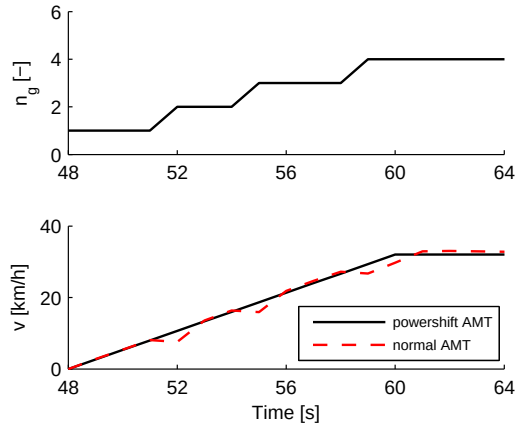


Figure 5: Zoom-in on NEDC of simulation results of powershift AMT vs. normal AMT.

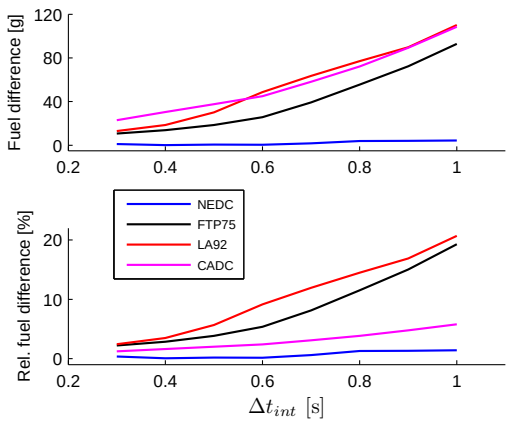


Figure 6: Sensitivity results of fuel difference with respect to a variation of interruption time $t_{int}$.

The results of a sensitivity study of the relative fuel difference (by comparing the fuel consumption of normal AMT with that of the powershift AMT) with respect to the variation of interruption time $\Delta t_{int}$ over the tested drive cycles is shown in Fig. 6. The interruption is varied as,

$$\Delta t_{int} \in \{0.3,\ 0.4,\ 0.5,\ 0.6,\ 0.7,\ 0.8,\ 0.9,\ 1\}[s], \tag{27}$$

to reflect the possible interruption time in a real gear shift. Herein $\Delta t_{int} = 0.3s$ represents the possible smallest time of actuating the synchronizer for a gear change. Meanwhile $\Delta t_{int} = 1s$ represents the longest interruption time for passenger cars. It notices that the slopes of the torque profiles during disengagement and engagement phases are unchanged for comfort reason. In this study, the slip time for each phase is chosen to equal 0.2s.
The relative traveled distances with both types of vehicle are almost identical ensuring that the drive missions for the normal AMT vehicle are completed on time.

- The results shown in Fig. 6 reveal that for longer interruption times, more fuel consumption results for the normal AMT vehicle compared with its powershift AMT counterpart. The results on drive cycles of FTP75, LA92 and CADC, representing real driving missions, demonstrate the superior fuel economy property of the powershift AMT compared to the normal AMT. Therefore, reducing the interruption time in the gear shifting process of the normal AMT would reduce fuel consumption with a considerable amount.

- On NEDC, the relative fuel consumption is very small and even equal to zero at $\Delta t_{int} = 0.4$. NEDC is a mild test drive cycle not representing a real drive pattern. However, from the fact of fuel equality of the driving profile resulted by the normal AMT in comparison with the original NEDC, it discloses a possibility of boosting fuel economy for HEVs by further optimizing the driving profile on a given driving distance and time constraints.

- In an attempt of explaining the rationale of the fuel benefit of the powershift AMT over the normal AMT, dynamical analysis of drive cycles is shown on Fig. 7. NEDC shows itself less dynamic and less realistic than the other drive cycles corresponding with a lowest relative fuel difference. LA92 possesses a highest dynamical property to result in a highest relative fuel difference, see Fig. 6. It can be concluded that, the more dynamic the drive cycle is, the more relative fuel difference the result is. Therefore drive cycles with many shifts required, e.g. driving in urban area, are fuel economy potential for the powershift AMT vehicle over the normal AMT vehicle.

- In commercial vehicles with normal AMTs, due to large drivetrain component inertias

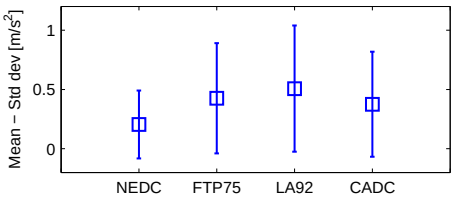


Figure 7: Dynamical analysis of drive cycle.

and reliable operation of transmissions, the interruption time is usually in order of 0.7-1.0s and larger. So, by looking at the results for $\Delta t_{int} = \{0.7,\ 0.8,\ 0.9,\ 1\}$, the average relative fuel differences on FTP75, LA92 and CADC are 7.7%, 10%, 12.2% and 15.3% respectively. Hence, it can be observed that fuel efficient for the powershift AMT over the normal AMT can be also held for commercial vehicle class.

Furthermore, by reflecting these saving amounts to other types of powershift transmissions, e.g. automatic and dual clutch transmissions, taking into account the intrinsic loss in the case of automatic [16] and friction loss of dual clutch slippage [17], it might be inferred that fuel economy benefits can be achieved with these powershift transmission applications wherein the interruption time of gear shift process is large, e.g. commercial vehicles. Nonetheless, simulation study for automatic and dual clutch transmissions is a prerequisite for supporting this general conclusion.

# 5 Engine Start Loss Model and Control Problem

## 5.1 Engine Start Loss Model

Full parallel HEV can utilize the electric machine positioned right after the clutch to start the engine. By exploiting this advantage, the parallel hybrid powertrain can eliminate the traditional engine starter. The starting process can be done through the chronological steps: 1) engaging the clutch to transmit torque from electric machine to accelerate the engine from zero to start speed; 2) after reaching the start speed, engine will takeover by combustion to synchronize its speed with the transmission input speed before fully engaging the clutch. Consequently, a decision of starting the engine would consume electric energy and fuel. Moreover in the step one of turning the engine up to its start speed, friction loss occurring in the clutch is also compensated through the electrical path. For simplification of modeling the start loss, friction loss in the step two can be neglected due to assumption of fast engaging the clutch at synchronization point.

In the context of designing an EMS, it can be assumed that the whole starting process occurs in one time step. Any decision to start the engine at any time step $k$ means that, the engine will be ready to propel the vehicle on the next time step $k + \Delta t$. The model of the engine start is graphically displayed in Fig. 8. Therefore, the involved loss models can be described as follows.

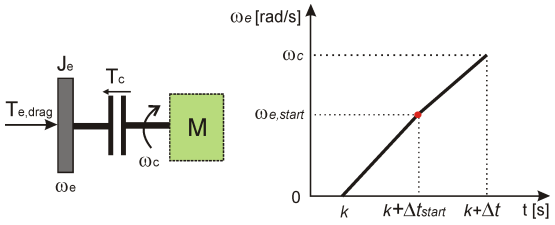


Figure 8: Engine start model.

### 5.1.1 Engine crank loss

we assume that the crank step can last within the average time interval $\Delta t_{start}$. The required torque from the electric machine for cranking the engine to start speed $\omega_{e,start}$ is the torque transferred through clutch $T_c$, defined as,

$$\begin{aligned} T_c &= J_e \frac{\omega_{e,start}}{\Delta t_{start}} + T_{e,drag}, \\ \Rightarrow \quad P_c &= \frac{\int_0^{\Delta t_{start}} T_c \omega_e dt}{\Delta t_{start}} = T_c \frac{\omega_{e,start}}{2}. \end{aligned} \tag{28}$$

wherein $T_{e,drag}$ is the engine drag torque.
The transferred torque $T_c$ is obtained by slipping of clutch which induces a friction loss. With a notation of clutch speed at the end of the starting process is $\omega_c$, the clutch friction loss is,

$$\begin{aligned} E_{c,loss} &= \int_0^{\Delta t_{start}} T_c\big(\omega_c - \omega_e\big) dt \\ &= \int_0^{\Delta t_{start}} T_c\big(\omega_c - \frac{\omega_{e,start}}{\Delta t_{start}} \cdot t\big) dt \\ &= T_c\big(\omega_c - \frac{\omega_{e,start}}{2}\big) \Delta t_{start} \end{aligned}$$

wherein $\omega_c = \omega_g$.
The averaged power loss at clutch,

$$P_{c,loss} = \frac{E_{c,loss}}{\Delta t_{start}} = T_c\big(\omega_c - \frac{\omega_{e,start}}{2}\big) \tag{29}$$

From (28) and (29), the total average required power placed at the electric machine,

$$P_{m,start} = P_c + P_{c,loss} \tag{30}$$

### 5.1.2 Synchronization loss

after reaching the start speed $\omega_{e,start}$, the engine takes over the synchronization with the transmission input speed by combustion. The energy loss can be derived from engine start power,

$$\begin{aligned} T_{e,start} &= J_e \frac{\omega_c - \omega_{e,start}}{\Delta t - \Delta t_{start}}, \\ \Rightarrow \quad P_{e,start} &= T_{e,start} \frac{\omega_c + \omega_{e,start}}{2}. \end{aligned} \tag{31}$$

It should be noticed that, the electric machine is assumed to operate under the nominal condition. Therefore even in the case of electrically driving, if engine start is required the surplus power from nominal to peak values can fulfilled the required power (30) for starting process.

## 5.2 Simulation Results

Table 3: Fuel economy study with gear shift hysteresis engine start loss are taken into account. Relative fuel is indicated in parathesis.

| Cycle | Baseline [g] | Hysteresis; Start loss [g] | Difference [g] | No. start [-] |
|---|---|---|---|---|
| NEDC | 300.5 | 303.1 | 2.6 (0.9%) | 14 |
| FTP75 | 480.3 | 489.9 | 9.6 (2%) | 85 |
| LA92 | 530.8 | 540.2 | 9.4 (1.8%) | 86 |
| CADC | 1873.9 | 1898.9 | 25 (1.3%) | 196 |

The engine start loss model is incorporated in the optimal control problem described in section 3. The gear shift hysteresis is active to avoid unrealistic shifting patterns. Simulation results are shown in Table 3. It can be seen that, compared to the baseline of no engine start loss and no gear shift hysteresis, the maximum relative fuel difference is 2% on FTP75; the minimum relative fuel is 0.9% on NEDC. Nonetheless, on CADC, the absolute different fuel is largest (25g) corresponding to largest number of start. Apparently, the more vehicle starts the engine, the more fuel is lost. Referring back to the simulation results of the gear shift hysteresis shown in Table 2, it can be recognized that, the engine start loss deteriorates fuel economy more than the gear shift hysteresis does.
In summary, the effect of engine start loss on fuel economy can not be ignored in seeking a fair evaluation of an economy hybrid vehicle.

# 6 Prediction Horizon Sensitivity Study

Losses involved with a discrete decision of either shifting gear or starting engine have been considered in the design of EMS to find out the theoretical value of fuel savings. However, knowledge of the whole drive cycle required for the designed EMS is almost impossible to obtain before driving. In reality, knowledge of a driving segment ahead the ongoing vehicle can be gained by prediction technique using the preview route information. Predictive control algorithm for hybrid powertrain systems appears to be a suitable candidate to realize a fuel saving level as much close to the theoretical value as possible.

## 6.1 Predictive Control Algorithm for Hybrid Powertrains

In this section, we use a certain drive cycle as a reference driving profile which is assumed to be constructed from consecutive preview route segments of the whole driving mission. The Model Predictive Control (MPC) problem for the prototype parallel HEV is formulated as follows.
Assuming that at current time step $k$ the prediction of vehicle speed $\tilde{v}(k) = \big[\hat{v}(k+1|k),\ \hat{v}(k+1|k),\ ...,\ \hat{v}(k+N_c|k)\big]^T$ is known over the horizon $N_c$, find an optimal control law $\tilde{u}^*(k) = \big[\tilde{u}^*_{se}(k),\ \tilde{P}^*_e(k),\ \tilde{u}^*_g(k)\big]$ that minimize the fuel cost functional $\hat{J}(k)$ over the entire prediction horizon.

$$\hat{J}(k) = \sum_{i=0}^{N_c-1} \dot{m}_f\Big(\hat{s}_e(k+i|k), \hat{P}_e(k+i|k), \hat{\omega}_e(k+i|k)\Big)\Delta t, \tag{32}$$

subject to the constraints (9) - (18) and,

$$E_{s\_min} \leq \hat{e}_s(k+N_c|k) \leq E_{s\_max}, \tag{33}$$

with

$$\hat{e}_s(k+N_c|k) = e_s(k) + \sum_{i=0}^{N_c-1} \hat{P}_s(k+i|k)\Delta t. \tag{34}$$

wherein: $\tilde{u}^*_{se}(k)$, $\tilde{P}^*_e(k)$ and $\tilde{u}^*_g(k)$ denote the vectors of predictive optimal solutions over the prediction horizon $N_c$ at time step $k$.
The MPC problem is solved by using the algorithm described in subsection 3.2. The predictive control approach is implemented in the receding horizon control manner to realize a real-time implementable algorithm when utilizing the predictive route information. Only the first element of the defined optimal trajectories of $\tilde{u}^*_{se}(k)$, $\tilde{P}^*_e(k)$ and $\tilde{u}^*_g(k)$ are applied to the hybrid powertrain system; for the next step $k+1$, the whole optimization process is repeated with the updated system states and new prediction of the route horizon.

The gear shift loss model can not be incorporated in the MPC due to the velocity loss at each gear shift resulting in the next vehicle speed dependent on gear position. Hence, we assume that the powershift AMT is equipped in the hybrid powertrain. The gear shift hysteresis and the engine start loss model are respect under the control problem design.

### 6.2 Simulation Results and Discussions

Sensitivity results of the relative fuel difference with respect to the prediction horizon $N_c$ are shown in Fig. 9. The relative fuel difference is obtained by comparing results of the MPC approach with that of the optimal control algorithm presented in section 3.
The baseline MPC, see the upper plot, indicates that with a short horizon of $N_c = 2$, the predictive controller realizes results very close to the optimal solution. The relative differences of fuel economy in steady state are very small, around 0.2%. However, for the case of the MPC with gear shift hysteresis and engine start loss model, from horizons $N_c = 4$ and larger, the relative differences of fuel economy are in steady state, ranged from 1% (NEDC) until 3% (FTP75). The obtained results reveal that at least a prediction horizon of 4s ahead the vehicle is necessary to achieve the most possible optimum fuel economy level. Fortunately, a prediction of velocity profile over a preview route segment with time length 4s is almost possible for current technology of vehicle onboard navigation system nowadays.
Sensitivity results of the calculation time with respect to the prediction horizon for the MPC strategy including the gear shift hysteresis and engine start loss is shown in Fig. 10. The calculation time is almost linear with the prediction horizon length and smaller than the drive cycle length itself. This brings a realtime implementation possibility to the MPC-based control algorithm.

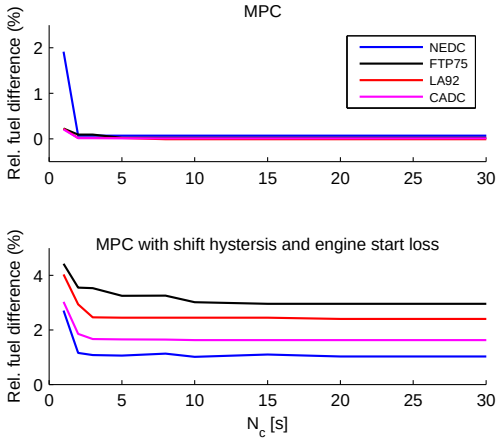


Figure 9: Sensitivity results of the relative fuel difference with respect to the prediction horizon $N_c$ of the MPC approach. Results of the baseline MPC is shown in the upper plot. Results of the MPC including the gear shift hysteresis and the engine start loss is shown in lower plot.

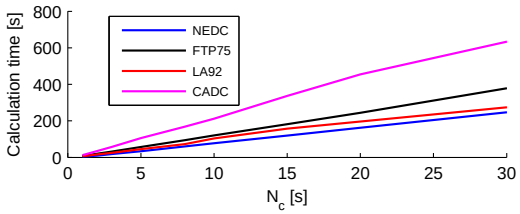


Figure 10: Sensitivity results of the calculation time for MPC approach with respect to the prediction horizon $N_c$.

## 7 Conclusions

Design of EMSs for passenger HEVs equipped with discrete-ratio transmissions required an optimal gear shift strategy for fuel economy benefit. One gear up or down per shift is the most optimum gear shift command in terms of fuel economy and engine operation comfort. Gear shift hysteresis strategy plays an crucial role in reducing the shift busyness and haunt in a way of not deteriorating fuel economy.
Regarding to the gear shift loss involved with a gear shift event, it has been found by simulation that a normal AMT hybrid vehicle suffers a significant fuel economy reduction when compared with a powershift AMT counterpart. It's too early to draw a general conclusion of fuel efficient advantage of a powershift AMT before experimental tests are carried out thoroughly. However, the wide margin of relative fuel savings of a powershift AMT over a normal AMT shown in this study can set a preliminary inference (in simulation) of fuel benefit of powershift transmissions, e.g. automatic, dual clutch or other types of powershift, over non-powershift transmissions for commercial vehicle application.
Any discrete decision of starting engine in a parallel HEV will induce a power loss which finally affects to the optimal solution and thus can not be ignored in the design of EMS. The model predictive control algorithm utilized the engine start loss model effectively in yielding the possible shortest prediction horizon such that the highest fuel economy level can be realized.
Prospects of future research are widely opened from this study. An investigation of the effect of gear shift engine start losses on the control strategies for a commercial vehicle equipped with an AT or dual clutch transmission is necessary. This helps to verify the fuel benefit of the powershift transmissions in comparison with the non-powershift ones in commercial vehicle class.

## Appendix: Vehicle Parameters

The main parameters of the HEV are given in Table 4.

Table 4: Main parameters of the HEV.

| Quantity | Descriptions |
|---|---|
| Diesel engine | maximum torque of 200Nm, maximum power of 68kW. |
| Electric machine | maximum torque of 20Nm, maximum power of 6kW. |
| Li-ion battery | capacity of 6Ah, 110V. |
| AMT | 6-speed type, $r_g = [3.817,\ 2.053,\ 1.302,\ 0.959,\ 0.744,\ 0.614]$. |
| Vehicle mass | 1320kg. |

## Acknowledgment

This study is part of the project 'Euro Hybrid' which is a research project of company Drivetrain Innovations B.V., together with the Eindhoven University of Technology, The Netherlands. The project is financially supported by Dutch government through AgentschapNL.

## References

[1] V. Ngo, T. Hofman, M. Steinbuch, A.F.A. Serrarens; Optimal Control of the Gear Shift Command for Hybrid Electric Vehicles; *IEEE Transactions on Vehicular Technology*, submitted October, 2011.

[2] V. Ngo, T. Hofman, M. Steinbuch, A. Serrarens; Predictive Gear Shift Control for a Parallel Hybrid Electric Vehicle; *2011 IEEE Vehicle Power and Propulsion Conference - IEEE VPPC 2011*, Chicago, USA, September 2011.

[3] T. Hofman, R.M. van Druten, A.F.A. Serrarens and M. Steinbuch; Rule-based Energy Management Strategies for Hybrid Vehicles; *Int. J. of Electric and Hybrid Vehicles*, vol.1, no.1, pages 71-94, 2007.

[4] M. Koot, J. T. B. A. Kessels, B. de Jager, W. P. M. H. Heemels, P. P. J. van den Bosch and M. Steinbuch; Energy Management Strategies for Vehicular Electric Power Systems; *IEEE Trans. Veh. Technol.*, vol. 54, pp. 771, May 2005.

[5] A. Sciarretta and L. Guzzella; Control of Hybrid Electric Vehicles: Optimal Energy Management Strategies; *IEEE Control System Magazine*, April 2007, pp 60-70.

[6] D. Ambuhl, O. Sundstrom, A. Sciarretta, L. Guzzella; Explicit Optimal Control Policy and its Practical Application for Hybrid Electric Powertrains; *Control Engineering Practice*, vol.18, no.12, pages 1429-1439, December 2010.

[7] N. Kim, S. Cha, H. Peng; Optimal Control of Hybrid Electric Vehicles Based on Pontryagin's Minimum Principle; *IEEE Transactions on Control Systems Technology*, vol. 99, pages 1-9, 2010

[8] D. Sinoquet, G. Rousseau and Y. Milhau; Design Optimization and Optimal Control for Hybrid Vehicles; *Optimization and Engineering*, DOI: 10.1007/s11081-009-9100-8, 2009

[9] J. T. B. A. Kessels, M. Koot, P. P. J. van den Bosch and D. B. Kok; Online Energy Management for Hybrid Electric Vehicles; *IEEE Trans. Veh. Technol.*, vol. 57, pp. 3428, Nov 2008.

[10] G. Rousseau, D. Sinoquet, P. Rouchon; Constrained Optimization of Energy Management for a Mild-Hybrid Vehicle; *Oil & Gas Science and Technology - Rev. IFP*, vol.62, no.4, pp.623-634, 2007.

[11] P. Pisu and G. Rizzoni; A Comparative Study of Supervisory Control Strategies for Hybrid Electric Vehicles; *IEEE Transactions on Control Systems Technology*, vol. 15, no. 3, May 2007.

[12] C. C. Lin, H. Peng, J. W. Grizzle, and J. M. Kang; Power Management Strategy for a Parallel Hybrid Electric Truck, *IEEE Trans. Control Syst. Technol.*, vol. 11, no. 6, pp. 839-848, Nov. 2003.

[13] S. Delprat, J. Lauber, T. M. Guerra, and J. Rimaux; Control of a Parallel Hybrid Powertrain: Optimal Control; *IEEE Trans. Veh. Technol.*, vol. 53, no. 3, pp. 872-881, May 2004.

[14] F. Wang, X.J. Mao, B. Zhuo, H. Zhong and Z.L. Ma; Parallel Hybrid Electric System Energy Optimization Control with Automated Mechanical Transmission; *Proc. IMechE, Part D: J. Automobile Engineering*, vol.222 no.4, pp.499-513, 2008.

[15] A. Sciarretta, M. Back, and L. Guzzella; Optimal Control of Parallel Hybrid Electric Vehicles; *IEEE Transactions on Control Systems Technology*, vol. 12, no. 3, pp. 352363, 2004.

[16] Leopold, R. D. ; A New Definition of Fuel Efficiency in Commercial Vehicles; *2009 SAE, Paper No 2009-26-026*

[17] O. Sundstrom, P. Soltic, L. Guzzella; A Transmission-Actuated Energy-Management Strategy; *IEEE Trans. Veh. Technol.*, vol.59, no.1, January 2010.

[18] L.Glielmo, L.Iannelli, V. Vacca, and F. Vasca; Gearshift control for automated manual transmissions; *IEEE Transactions Mechatronics*,vol. 11, no. 1, pp. 17-26, 2006

[19] D. G. Florencio, E. R. Assis C. H. F.Amendola;The Manual Transmission Automated - Gearshift Quality Comparison to a Similar Manual System; *2004 Society of Automotive Engineers.*

[20] M. Yamasaki, H. Konno, H. Kuroiwa, N. Ozaki; Automated Manual Transmission with Torque Assist Mechanism for Reducing Shift Shock; *2005 SAE International.*

[21] D. V. Ngo, T. Hofman, M. Steinbuch, A. Serrarens; An Optimal Control-Based Algorithm for Hybrid Electric Vehicle Using Preview Route Information; *In Proceeding of 2010 American Control Conference - ACC2010*, Maryland-USA, June 2010.

[22] T. van Keulen, B. de Jager, and M. Steinbuch; Optimal Trajectories for Vehicles with Energy Recovery Options; *Proceedings of the 18th IFAC World Congress*,2011.

[23] L. Guzzella and A. Sciarretta; *Vehicle Propulsion Systems: Introduction to Modeling and Optimization*; Springer, the 2nd edition, 2007.

[24] D. P. Bertsekas; *Dynamic Programming and Optimal Control*, 2nd edition; Athena Scientific, 2002.

[25] Drivetrain Innovations B.V.; Powershift Automated Manual Transmission (PS-AMT); www.dtinnovations.nl

## Authors

**Viet Ngo** received the M.Sc. degree in Mechanical Engineering from Sungkyunkwan University, South Korea in 2007. Since May, 2008 he has been a Ph.D. candidate with Control Systems Technology group, Eindhoven University of Technology, The Netherlands. His research interests are modeling and control of hybrid vehicle propulsion systems. In 2011, he received the 'Best Paper Prize' at the IEEE Vehicle Power and Propulsion Conference 2011 (VPPC2011), Chicago, USA.

**Theo Hofman** received his Ph.D. degree in 2007 at Eindhoven University of Technology, The Netherlands. Since 2010, he is an Assistant Professor with the Control Systems Technology group, Mechanical Engineering Dept, Eindhoven University of Technology in the field of vehicle propulsion systems. The current research focusses on methods for combined control and system design optimization within the application field of propulsion systems.
Since 2004, he has been an International Program Committee member of the IEEE Vehicle, Propulsion and Power Conference (VPPC). Since 2006, he is also an Associate Editor of the Int. J. of Hybrid and Electric Vehicles (IJEHV). In 2006, he received the Youth Paper Award for his contribution to the 22nd International Battery, Hybrid and Fuel Cell Electric Vehicle Symposium & Exposition in Japan.

**Maarten Steinbuch** received the Ph.D. degree in 1989 from Delft University of Technology. Since 1999 he is full professor in Systems and Control, and head of the Control Systems Technology group of the Mechanical Engineering Department of Eindhoven University of Technology. He is the Editor-in-Chief of IFAC Mechatronics and associate editor of Int. Journal of Powertrains. He is program leader of the TU/e Master of Science Automotive Technology. Since july 2006 he is also scientific director of the center of Competence High Tech Systems of the Federation of Dutch Technical Universities. His research interests are modeling, design and control of motion systems, robotics, automotive powertrains and control of fusion plasmas.

**Alex Serrarens** received his PhD degree from Eindhoven University of Technology, The Netherlands, in 2001 in the field of powertrain control of passenger cars with CVT. Currently, he is business partner within Drivetrain Innovations B.V. (DTI with url: www.dtinnovations.nl) which is a licensing and contract-research center on automotive powertrains, transmissions, and components.